RSC Advances

ROYAL SOCIETY OF CHEMISTRY

www.rsc.org/advances

Cite this: DOI: 10.1039/c0xx00000x

www.rsc.org/xxxxxx

ARTICLE TYPE

Bioinspired protein microparticles fabrication by peptide mediated disulfide interchange

Kwok Kei Lai,[a] Reinhard Renneberg [a] and Wing Cheung Mak *[b,c]

Received (in XXX, XXX) Xth XXXXXXXXX 20XX, Accepted Xth XXXXXXXXX 20XX

DOI: 10.1039/b000000x

In this article, we report an innovative green chemistry approach for the fabrication of protein microparticles based on peptide mediated disulfide interchange reactions. The concept is based on using a redox reactive peptide, glutathione, as a natural crosslink reagent triggers the formation of intermolecular disulfide bonds between adjacent protein molecules leading to the assembly of protein molecules within a $CaCO_3$ template into microparticle structure. The $CaCO_3$ template is highly biocompatible and is completely removed by simply adjusting the solution to pH 5.0, leaving behind the pure protein microparticles. Moreover, the GSH only involved in the intermediate step without being incorporated into the resulting protein microparticles, therefore producing protein microparticles composed of purely protein molecules. This technology provides a simple and robust method to fabricate protein microparticles at physiological aqueous condition, and more importantly avoiding the extensive use of synthetic chemical crosslinking reagents. We have further demonstrated this method is versatile to fabricate microparticles with various proteins such as BSA, enzymes and antibodies. The biological functions such as catalytic properties and affinity interaction of the resulting protein microparticles are highly conserved which demonstrate the potential applications of the protein microparticles in the area of biocatalysis, bioseparation and targeted drug delivery.

Introduction

Scientists are looking for new biomaterials particularly in microparticle formulation for emerging medical, pharmaceutical and biological applications [1–6]. Proteins are excellent natural building block to prepare microparticles due to theirs versatile functionalities and good biocompatibility [7]. Many works have been focused on the preparation of protein microparticles with controlled size distribution, porosity and composition [7,8]; while the extensive use of synthetic crosslink chemicals during the fabrication process remains one of the major challenges for bringing such protein microparticles for practical biomedical applications.

In general, most of the conventional methods described on the preparation of protein microparticles involve firstly the formation of protein micro-compartments via spray drying [9], emulsification[10] or template entrapment techniques [11]; and subsequently covalent crosslink the protein molecules within the micro-compartments using synthetic crosslink reagents such as glutaraldehyde or EDC/NHS [12,13]. These chemical approaches were fast and potent, but yet they brought about safety concern when applying the resulting protein microparticles for *in vivo* researches [14]. Most of the synthetic amine reactive crosslink reagents were known to be toxic and would trigger allergic reactions in animals [15]. More importantly, the mechanism of these chemical crosslink reagents usually involves coupling reactions between amine groups and carboxyl groups in proteins that results in alternating the isoelectric property of proteins which may affect the biological functions of the resulting protein microparticles.

In nature, biomolecules are assembled into complex macromolecular structures having fibrous or globular morphology through covalent and non-covalent biomolecular interactions. Fibrillin-rich microfibril is an example of complex thin filament composed of assembled fibrillin molecules that presence virtually in all connective and elastic tissues [16,17]. Disulfide interchange has been proved as one of the key mechanism mediating the assembly of fibrillin into microfibrils by the formation of intermolecular disulfide bonds between adjacent fibrillin molecules [18]. It is also suggested the intermolecular disulfide bonds between fibrillins are essential contributing to the unique elastic biomechanical property of the microfibrils which is significant for connective tissues [19]. Another example is the intracellular storage of thyroglobulin which is a secretory protein from exocrine glands serves as a precursor of thyroid hormone. Storage of thyroglobulin has significant physiological means to provide a reservoir for regulating the level of thyroid hormone upon utilization by the organism [20]. The cellular storage of thyroglobulin is accomplished by molecular assembly of thyroglobulin molecules into globular structure by mainly formation of intermolecular disulfide bonds between thyroglobulin molecules driven by either enzyme isomerase or disulfide interchange reaction [20,21]. The thyroglobulin globules

allow storage of thyroglobulin reaching a high concentration of up to 800 mg mL^{-1} in an osmotically inert form [22].

In this paper, we present a bioinspired biochemical approach for the fabrication of protein microparticles based on template-assisted protein assembly via formation of intermolecular disulfide bonds. This new concept is based on mimicking the intracellular disulfide interchange reactions at physiological conditions mediated by glutathione as a natural reducing agent (antioxidant) presents in cells. Glutathione (GSH) is a redox-active tripeptide composed of three amino acids: glutamate, cysteine and glycine synthesize within cells with a physiological concentration of approximately 5 mM [23]. GSH has diverse physiological roles such as to prevent the elevation of oxidative stress that can damage the cell components, including critical genetic components such as DNA and RNA [24,25], regulation of cellular proliferation and apoptosis and the post-transcriptional modification of proteins through S-glutathionylation, as well as mediation of cellular assembly of biomolecules [26]. The mechanisms of these physiological roles are mainly driven by the potent redox capability of GSH via disulfide interchange reactions [27].

In brief, the protein microparticles fabrication involves entrapment of protein molecules e.g. bovine serum albumin (BSA), enzyme or antibodies inside spherical calcium carbonate ($CaCO_3$) template by coprecipitation. GSH was then added to trigger disulfide interchange reactions between protein molecules. After washed away the GSH, the entrapped protein molecules form new intermolecular disulfide bonds with the adjacent protein molecules constructing the 3-dimensional protein network. Finally, the $CaCO_3$ templates were removed by reducing the buffer pH to 5 and pure protein microparticles were produced (Fig. 1). The kinetic of the disulfide exchange reactions and the degree of intermolecular disulfide crosslink within protein microparticles were studied. Protein microparticles composed of functional proteins such as enzymes and antibodies were fabricated with preserved enzymatic activities and affinity interactions. These results demonstrated an innovative green chemistry approach to fabricate functional protein microparticles with potential applications in the areas of pharmaceutics, bioseparation and biocatalysis.

Experimental

Materials

Bovine serum albumin (BSA), 3,3,5,5-tetramethylbenzidine dihydrochloride (TMB), and horseradish peroxidase (HRP) was purchased from Sigma. Dithiotheritol (DTT), calcium chloride, sodium carbonate and L-Glutathione reduced were purchased from Sigma-Aldrich (Missouri, USA). UltraPure™ Ethylenediaminetetraacetic acid (EDTA) was purchased from Invitrogen (Carlsbad, CA, USA). Low Viscosity Spurr Formula Kit I was purchased from SPI-Chem (West Chester, PA, USA). Total Glutathione Detection Kit (ab65324) was purchased from Abcam (Cambridge, England). Hydrogen peroxide (H_2O_2) was purchased from Honeywell Riedelde Haën (Seelze, Germany). Affinity-purified polyclonal goat anti mouse immunoglobulin G (GtαM-IgG) and mouse immunoglobulin G (M-IgG) were purchased from Arista Biologicals Inc. (Allentown, PA, USA).

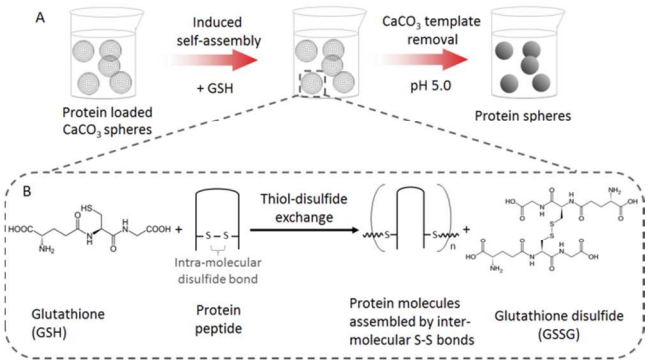

Fig. 1 A) Schematic diagram illustrating the fabrication process for the protein particles. B) Outline of the peptide mediated disulfide interchange chemistry to induce assembles of protein molecules into microparticles.

Preparation of protein microparticles

Preparation of protein microparticles were performed by co-precipitation reaction entrapping protein molecules into $CaCO_3$ microparticles (templates) [28], followed by disulfide interchange reaction induced by glutathione (antioxidant present in cells). In brief, calcium chloride (0.5 M) and sodium carbonate (0.5 M) are mixed rapidly in the presence of BSA (10 mg mL^{-1}) inside a beaker with magnetic stirrer. After mixing for 30 seconds, the mixture containing calcium carbonate and entrapped BSA was collected and washed by centrifugation (3600 r.p.m., 1 min) and redispersion cycles with double distilled water for 5 times to remove excess BSA from the template. The $CaCO_3$ template loaded with BSA were incubated with glutathione solution with concentration ranged from 0.001 to 5 mM at pH 7.5 for 30 min. The glutathione solution was freshly prepared by dissolving anhydrous glutathione in double distilled water prior to use. Subsequently, excess glutathione was removed by centrifugation (3600 r.p.m., 1 min) and redispersion cycles with double distilled water for 5 times, and incubated for 1 hour at room temperature. Finally, the $CaCO_3$ template was removed by either addition of EDTA (0.2 M) and incubated for 15 minutes; or by acid titration with hydrochloric acid to pH 5. The resulting pure BSA microparticles were washed twice by centrifugation (5000 r.p.m., 2 min) and redispersion cycles.

Quantification of glutathione concentration

In theory, GSH will reduce disulfide bonds by losing a hydrogen atom. After that it reacts with another glutathione molecule to form the oxidized dimeric form, GSSG. This change in chemical structure was detected by o-phthaldialdehyde (OPA), which is a fluorescence probe sensitive for the detection of SH groups quantifiable by spectrophotometer. The glutathione concentration as a function of time during the fabrication process was quantified using Total Glutathione Detection Kit (ab65324, abcam). Briefly, during the glutathione incubation process, 100 µL reaction mixtures were collected at different time intervals, followed by centrifugation (3600 r.p.m., 1 min). 60 µL of the supernatant was collected and stabilized by addition of perchloric acid immediately. After incubated for 5 min, 20 µL KOH (3N) was added to 40 µL of the mixture for neutralization. The mixture was spun down by centrifuge (13,000 r.p.m., 2 min, 4 °C) to

retrieve the supernatant. 10 µL of the neutralized solution was transferred to a well in microtiter plate and mixed with 90 µL of the supplied assay buffer. Finally, 10 µL of the OPA probe from the kit was added and incubated in dark at room temperature for 40 min. The fluorescent intensity was then quantified by spectrophotometer (FLUOStar OPTIMA, BMG LABTECH) at Ex/Em = 350/470 nm. Control experiments measuring glutathione concentration in the absence of microparticles were performed with the same experiment conditions.

Quantification of enzyme kinetics for peroxidase microparticles

Peroxidase microparticles were prepared under the same procedures as described above with modified ingredients. BSA-HRP conjugates were prepared according to the protocol of EDC-NHS coupling. In brief, a solution mixture containing 960 µL BSA solution (2.08 mg mL^{-1}), 20 µL EDC, and 20 µL NHS in 0.1 M MES buffer (pH 6.0) was freshly prepared and incubated for 15 min at room temperature to activate the BSA. 1 mL HRP solution (~770 units mL^{-1}) was then added to the activated BSA solution mixture followed by an incubation of 2 h at room temperature under continuous mixing by Rotator Mixer RM-Multi 1 (Starlab Group, Germany). Subsequently, the BSA-HRP conjugates were harvested and washed using 50K Nanosep® centrifugal device (Pall, USA). The conjugates were concentrated to a final volume of 100 µL. In the next step, 40 µL of the conjugates was included alongside with BSA as the enzymatic component of the microparticles.

Enzyme kinetics of the resultant BSA-HRP microparticles were studied by means of colorimetric reaction between HRP and its specific substrate 3,3',5,5'-tetramethylbenzidine (TMB) in the presence of an oxidizing agent, H_2O_2. In brief, 40% TMB working solution was prepared by mixing TMB (1 mg mL^{-1} in DMSO) with 0.1M phosphate-citrate buffer at pH 5.0. H_2O_2 was freshly added before using in a final concentration of 0.035%. A series of 0.5x dilutions starting with 40% TMB working solution was prepared in 8 successive wells on microtiter plate. The volume of diluted TMB working solution in each well equaled to 100 µL and the same volume of BSA-HRP microparticles was added simultaneously using multichannel micropipette. The microtiter plate was immediately read by spectrophotometer (FLUOStar OPTIMA, BMG LABTECH) with absorbance at 380 nm over time for quantifying the blue color product generated from the reaction between the enzyme and TMB. Control experiments quantifying the kinetics of free HRP in the absence of microparticles were performed with the same experiment conditions.

Initial rates of enzymatic reaction for different substrate concentrations were calculated from the absorbance data. For both microparticles and free HRP, Michaelis-Menten model was applied for obtaining the enzyme kinetics, which is a generally accepted model for calculation. The initial rates of reaction (V_i) were plotted against the substrate concentrations ([S]). The maximum rate of reaction (V_{max}) was drawn from the curve at the saturation point. Then the Michaelis constant (K_m) was found graphically from the x-axis at the point where the rate of reaction equals to half V_{max}.

Quantification of affinity interaction for antibodies microparticles

Antibodies microparticles were prepared under the same procedures as described above with modified ingredients. Goat-anti-mouse immunoglobulin G (GtαM-IgG) in a concentration of 10 mg mL^{-1} was included alongside with BSA as the antibody component of the microparticles. The resultant BSA-GtαM-IgG microparticles were harvested for characterizing their affinity interaction with corresponding antigens using qNANO (Izon, New Zealand). The equipment used tunable resistive pulse sensing (TRPS) technique to get particle information on particle-by-particle basis. The diameters of microparticles before and after reacting with different analytes were measured and analyzed. In brief, 30 µL of BSA-GtαM-IgG microparticles suspended in 20 mM Tris buffer (pH 8) was injected to qNANO for measuring their size. Subsequently, 10 µL of mouse IgG (9.8 mg mL^{-1}) or rabbit IgG (10 mg mL^{-1}) in the same Tris buffer was added to mix with the microparticles. The sizes of particle before and after the addition of different analytes was recorded and analyzed by the bundled software "Izon's control suite" v2.2.

Characterizations

Scanning electron microscopy (SEM) was used to reveal the morphology of the microparticles. For studying surface morphology, microparticle samples were washed by double distilled water for 3 times and then dropped onto silicon wafer affixed on copper stand with conducting silver metal paint. For revealing the inner structure of the microparticles, they were first embedded in resin using Spurr Formula Kit I, then cross-sections with thickness between 2 - 5 µm were obtained by rotary microtome (Leica, Germany). The SEM images were recorded with JSM-6700F or JSM-7100F (JEOL, Japan) at 5 kV or 10 kV, respectively. The presence of calcium carbonate template in microparticles after treatment with EDTA and acid titration was done by energy-dispersive X-ray spectroscopy using INCA X-ray Microanalysis system (Oxford Instruments, UK) coupled on scanning electron microscope JSM-6300 (JEOL, Japan). The number of microsparticles was counted with the aid of Bright-Line Hemacytometer (Reichert-Jung, Buffalo, New York, USA). Fourier Transform Infrared (FTIR) study was performed with VERTEX 70 (Bruker, USA) equipped with a germanium attenuated total reflectance (ATR) sample cell. BSA-HRP solution (10 mg mL^{-1}) and BSA-HRP microparticles suspension (~10^9 microparticles mL^{-1}) were dropped onto the surface of the ATR cell and FTIR spectra were recorded in the frequency region of 600-4000 cm^{-1} with a resolution of 4 cm^{-1} and run for 100 cycles.

Results and discussion

Optimum glutathione concentration for protein microparticles formation

Glutathione is a natural peptide driven the disulfide interchange reaction which influence the degree of crosslink between protein molecules and the morphology of the resulting protein microparticles. A series of protein microparticle samples were fabricated with various amount of glutathione ranging from 0.001

mM to 5.0 mM, and their surface morphologies were examined using SEM. The highest glutathione concentration was chosen at 5.0 mM, which is equivalent to the normal physiological value found in animal cells [23]. Fig. 2 shows pure protein microparticles were obtained with glutathione concentration above 0.01 mM, while no microparticles found with glutathione concentration below 0.001 mM (data not shown). The morphology of the protein microparticles shows a three-dimension spherical structure at high glutathione concentration above 0.5 mM (Fig. 2A-2D); while the microparticles appeared flattens when the glutathione concentration below 0.1 mM (Fig. 2E-2F). In addition, the measured diameters of the protein microparticles in the SEM images increased from about 2.1 μm to 4.1 μm as the microparticles morphology become flattened at low glutathione concentration. These observations could collectively be explained by the degree of disulfide interchange and the formation of inter-molecular disulfide bonds between protein molecules. As the glutathione concentration increased, the degree of disulfide exchange is higher which produces more free-cysteine groups within the protein molecules available forming inter-molecular disulfide bonds. Therefore, the degree of crosslinking between protein molecules is higher which resulting the formation of three-dimensional intact protein microparticles. In contrast, protein microparticles fabricated with lower glutathione concentration were collapsed and spread during the drying process for imaging, therefore appeared with increased diameter and flatten morphology. For this context, a glutathione concentration of 2 mM was chosen for future experimental condition.

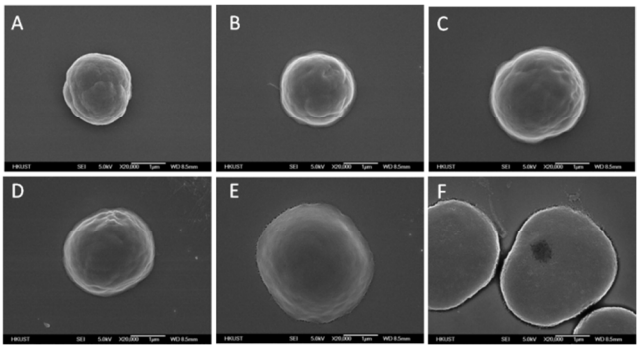

Fig. 2 SEM images of protein microparticles produced with GSH concentration at (A) 5 mM; (B) 2 mM; (C) 1 mM; (D) 0.5 mM; (E) 0.1 mM; and (F) 0.01 mM, respectively.

The efficiency of GSH as naturally occurred antioxidant was compared with one of the most commonly used artificial antioxidant dithiothreitol (DTT). The morphology of protein microparticles produced using GSH (2 mM) and DTT (2 mM) looks almost identical (Fig. S1). However, the GSH reaction required 30 minutes incubation time to obtain protein microparticles, while DTT reaction required only 10 minutes incubation time. This can be explained from the chemical structural difference between GSH and DTT. DTT possesses two thiol groups per each molecule. When either of the thiol group became oxidized by losing an hydrogen atom from thiol-disulfide interchange reaction, the intermediate form was unstable that makes the second thiol group have high tendency to release the hydrogen atom and form a more stable closed ring structure. In another words, every DTT molecule is capable of performing two thiol-disulfide interchange reactions. In contrast, GSH having only one thiol group per each molecule which is estimated to be less potent than DTT in the reducing power. Although DTT is more efficiency for protein microparticles production, studies have shown that DTT could induce apoptosis in HL-60 cells and Eca-109 cells [29,30]. Regardless of the fact that both DTT and GSH can be washed away after the fabrication process, using GSH as a natural chemical source could offer a safer and biocompatible process for fabrication of protein microparticles, more importantly to reduce the use of potentially harmful chemicals such as DTT during the fabrication process leading to disposal problem, as well as to minimize the chance of contamination from the intermediate hazardous reactants due to incomplete washing process making our protein microparticles more friendly for pharmaceutical and biomedical applications.

Proof of disulfide interchange and protein microparticles formation

The principle of protein microparticle formation is based on disulfide exchange reaction. During the microparticle formation, GSH was acted as a reducing agent donating hydrogen atoms to open the intra-molecular disulfide bonds of protein molecules and forming free thiol groups, while the GSH was converted into glutathiyl radical (GS*). The GS* will then stabilizes itself by reacting with another GSH forming the oxidized dimeric glutathionine disulfide (GSSG). The reactive thiol groups within the protein molecules then form new inter-molecular and intra-molecular disulfide bonds to complete the disulfide exchange reaction.

In order to proof and monitor the kinetics of the disulfide exchange reactions, the concentration of GSH was measured as a function of incubation time. For this study, the concentration of GSH used was reduced to 0.5 mM so that the GSH becomes the limiting factor, which the consumption of GSH for the disulfide exchange reactions were measured. Fig. 3 shows a significant decrease in the GSH concentration of 52% within the first 10 minutes incubation followed by an observation of a slightly decreasing trend. The decrease in GSH concentration is likely due to the convention of GSH into GSSG during the disulfide exchange reactions. Control experiment was performed showing a constant GSH concentration over time, which demonstrated the decrease in GSH concentration during microparticle fabrication was not due to self-decomposition. Moreover, a further control experiment was performed in which no GSH was added to the microparticle suspension. The signal of GSH was undetectable (Data not shown). These results implied there was neither interference nor background signal coming from the BSA and calcium carbonate template. Thus the decrease in GSH concentration was significantly contributed by the disulfide exchange reaction between GSH and BSA.

By calculating the consumption of GSH during the fabrication process, the degree of crosslinking within protein microparticles were evaluated. The degree of protein crosslink was defined as the total number of inter-molecular disulfide bonds per unit volume. The calculation is based on the following assumptions: 1) two GSH molecules were consumed to split a disulfide bond into two free thiol groups, 2) the efficiency of the disulfide exchange reaction by GSH is 100%, and 3) each available intra-

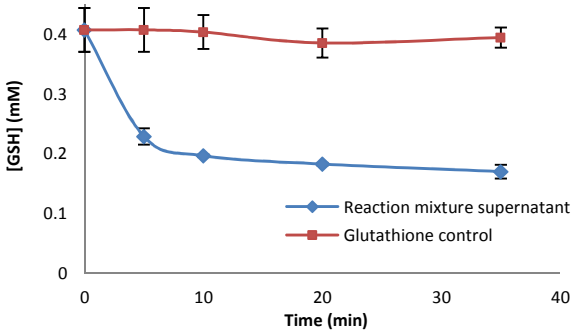

Fig. 3 A graph showing the consumption of glutathione resulting from disulfide interchange reaction as a function of time.

molecular disulfide bond undergoes only one disulfide exchange reaction and forming a new inter-molecular disulfide bond.

By considering a reaction volume of 1 mL, the amount of GSH consumed during the disulfide exchange reaction was 0.22 mM according to Fig. 3, which is equivalent to 2.2 x 10^{-7} moles of GSH. Since two GSH is required to split one disulfide bond producing two thiol groups, the number of free thiol groups produced is equal to 2.2 x 10^{-7} moles. Assuming two free thiol groups will lead to the re-formation of one new inter-molecular disulfide bond crosslinking the protein molecules, the total number of protein crosslink groups was calculated to be 1.1 x 10^{-7} times Avogadro's constant (6.02 x 10^{23}), which is equal to 6.6 x 10^{16}. With the aid of hemacytometer and optical microscope, the total number of microparticles per milliliter solution was calculated to be 2.1 x 10^{9}. The mean radius of the microparticles measured from the SEM images is about 1 μm (n=10). The volume of each microparticles is about 4.2 μm^3. Based on the above calculations, the degree of protein crosslink was calculated as: (Total number of inter-molecular disulfide bonds)/(Total number of microparticles)/(Volume of each microparticles), which is equal to 7.5 x 10^{6} disulfide bonds per unit μm^3.

Morphological characterization of protein microparticles

The $CaCO_3$ templating method allows the fabrication of protein microparticles with well-defined sizes, as well as controlled internal structures, which is highly desired especially for pharmaceutical applications. The porous structure of the $CaCO_3$ template is consisted of vaterite crystal structure having inter-connected pores with uniform size of about 10-30 nm [31]. During the protein microparticle fabrication process, protein molecules were entrapped within the pores of the $CaCO_3$ template, followed by inter-molecular crosslink forming the microparticles. Fig. 4 shows a high resolution SEM image of the protein microparticles. The protein microparticle was composed of assembled granular structure with size of tens of nanometers (Fig. 4A), which is likely contributed by the porous nature of the $CaCO_3$ template. In order to proof that the granular structures are the primary modules forming the protein microparticles, we further examined the inner structure of the microparticles in $CaCO_3$ template (Fig. 4B). The cross-section of the protein microparticles shows a fairly uniform granule structures in a radiating pattern were observed within the inner core of the microparticles. The radiating pattern is a result of the growth of the $CaCO_3$ template during the co-precipitation process started from the center towards the edge. The removal of $CaCO_3$ at the end of the fabrication process left the protein microparticles as highly porous structure.

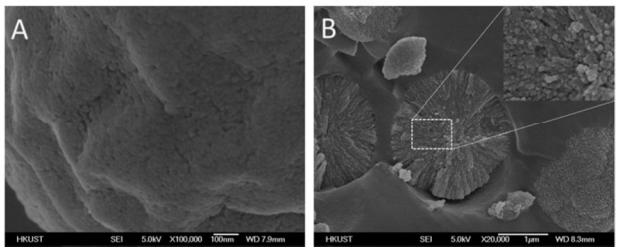

Fig. 4 Scanning electron micrographs showing (A) surface of protein microparticle, and (B) cross-sectional image of microparticles in $CaCO_3$ template. Assembled granules structure with size of tens of nanometers was found both on the surface and inner core of the protein microparticles.

In parallel to SEM imaging, energy-dispersive X-ray spectroscopy (EDX) was performed to characterize the element composition of the protein microparticles before and after $CaCO_3$ template removal. Upon X-ray irradiation, the back scattered spectrum was collected and analyzed for the elements that are present on the sample. Before $CaCO_3$ template removal, the EDX spectrum shows a considerable amount of calcium content, contributing to about 23% (Fig. 5A). While, after $CaCO_3$ template removal by acid titration to pH 5, the calcium content were not detectable within the protein microparticles (Fig. 5B). It should be noted that the EDX analysis was not limited to the surface of the microparticle samples. With a 10 keV primary electron beam, the penetration depth can go down to approximately 3 μm [32], which provides a deep analysis into the core of the microparticles. This result demonstrates by adjusting the pH value to 5.0 with acid titration is effective for complete removal the $CaCO_3$ template, and the microparticles produced are composed of purely protein molecules.

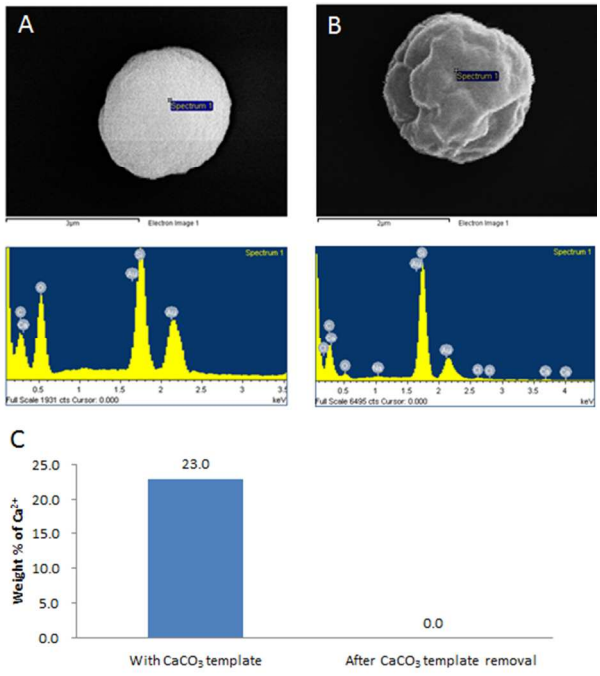

Fig. 5 EDX spectrum of (A) protein microsparticles in $CaCO_3$ template and (B) pure protein microparticles after CaCO3 template removal. (C) The bar chart shows the percentage weight of calcium in both samples indicates a complete removal of $CaCO_3$ template by simply adjusting the solution to pH 5.0.

Enzymatic and affinity functions of the protein microparticles

In order to demonstrate protein functions are conserved within the microparticles fabricated with the disulfide exchange process, protein microparticles composed of enzyme and antibodies were fabricated, which their enzymatic activities and affinity interactions were evaluated. For enzymatic activities studies, hybrid protein microparticles composed of horseradish peroxidase (HRP) and BSA (BSA-HRP microparticles) was chosen as a model. HRP is a heme protein consists of a total number of 309 amino acids with 8 cysteine residual on each subunit that corresponds to 2.6% cysteine content (primary sequence available from NCBI database). The three dimensional structure of the HRP molecules suggested the possible accessibility of the cysteine residuals for disulfide interchange reactions located near to the surface of the enzyme structure (Fig. S2). It is well known that the activity of an enzyme is highly correlated to their structural conformation which forms a catalytic active site converting a specific substrate to a product [33]. A change in the structural conformation as a result of protein denaturation will affect the enzyme catalytic functions, which influences the rate of substrate-product conversion reaction. The BSA-HRP microparticles were incubated in a buffer solution containing hydrogen peroxide and chromogenic substrate 3,3',5,5' -Tetramethylbenzidine (TMB). The enzyme HRP within the microparticles catalyzed the oxidation of TMB in the presence of hydrogen peroxide forming a product with a characteristic blue colour which can be quantitatively measured by spectrophotometer at 650 nm. The enzyme kinetics of the BSA-HRP microparticles were measured and compared with the free HRP. For this study, Michaelis-Menten kinetics from both test cases were derived from the hyperbolic curves where the rates of reaction were plotted against different substrate concentrations.

The maximum reaction rate (V_{max}) of BSA-HRP microparticles shows a 10.6% decrease compared with free HRP, while for the Michaelis constant (K_m), the obtained value from BSA-HRP microparticles resulted in a 9% increase over the free enzyme (Fig. 6). A higher K_m value indicates a lower affinity between the enzyme and the substrate. This result may be explained by the slight conformational changes in enzyme active sites resulted from the disulfide exchange reactions and formation of intermolecular disulfide bond after microparticle formation. In addition, protein molecules are assembled in close proximity within the particle which created a physical barrier limiting substrate diffusion. These affect the enzyme-substrate affinity and in turn slowed down the apparent reaction rate which resulted in a lower V_{max} value for the BSA-HRP microparticles compared with free HRP in solution. Nevertheless, it should be noted that the kinetics difference is only about 10% between the BSA-HRP microparticles and the free HRP. These suggested the disulfide interchange reaction mediated by glutathione only slightly influenced the enzymatic function, and the protein conformation reflected by the enzyme kinetic is mostly conserved.

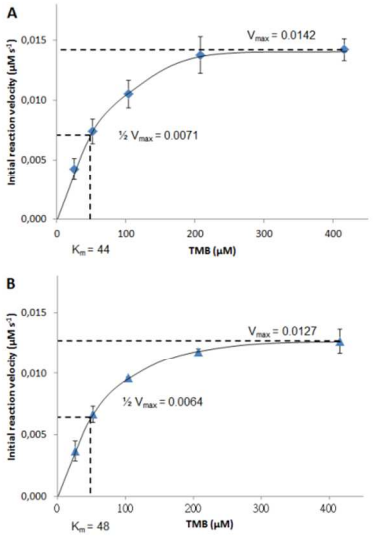

Fig. 6 Hyperbolic curves of (A) free HRP, and (B) BSA-HRP microparticles for the determination of Michaelis-Menten kinectis with initial reaction rate plotted against substrate concentration.

In addition, FTIR spectroscopy was used to study the structural integrity of the BSA-HRP solution and BSA-HRP particle suspension. The structural features of proteins such as α-helix and β-sheet can be interpreted through amide I and amide II bands in the region of 1700-1600 and 1600-1500 cm^{-1}, respectively [34]. The FTIR spectra of native BSA-HRP solution and the BSA-HRP microparticles are similar and no significant spectral shifting for the protein amide I band and amide II band was observed (Fig. S3). In addition, the area ratio of the amide I band and amide II band of the native BSA solution and the BSA microparticles are similar. This indicates the percentage of the α-helix and β-sheet structures presence in the native protein molecules and the protein molecules within the microparticles agree with each other. This result may suggest the secondary structure of the protein molecules within the microparticles resembles the native molecules. However, the FTIR results can only demonstrate the protein structural integrity at the level of secondary conformation, while the structural integrity on the tertiary and quaternary structure of the of the BSA-HRP molecules within the BSA-HRP microparticles is still unclear. We suggested the formation of new intermolecular disulfide bonds crosslinking the protein molecules will lead to a change in the structural integrity of the protein molecules, our results demonstrated these changes will not significantly affect the protein function and the biological activities of the enzyme are conserved. This may be explained by the presence of other forces such as hydrophobic interactions, hydrogen bonds, and *val der Waals'* forces are involved in the stabilization of the protein structure and protein function. We further attempted to characterize the iron content of the BSA-HRP microparticles using energy-dispersive X-ray spectroscopy (EDX). HRP has a molecular weight of ~44,000Da, while the Fe ion has a molecular weight of 55.8. The percentage of iron is only 0.13% of the total mass of the HRP molecule. Therefore, it is difficult to measure accurately the iron content of the HRP-BSA microparticles. Since HRP is an iron heme protein, the conserved enzymatic activity of the BSA-HRP microparticles may suggest the iron content within HRP molecules is retained.

Apart from enzyme, antibody was chosen as an alternate model to evaluate if there is any critical change in the protein function after microparticle formation. The conformation of the epitope of antibodies determines the specific affinity with their target antigen. Any distortion in the binding grove may result in the loss of affinity or lead to cross-reactivity with non-specific antigens [35]. In this study, goat-anti-mouse immunoglobulin G (GtαM-IgG) was blended with BSA for fabricating of BSA-GtαM-IgG microparticles as a study model. The microparticles were allowed to incubate with mouse immunoglobulin G (M-IgG), the specific antigen for GtαM-IgG. The affinity binding between the antibodies present on the microparticles and M-IgG was reflected by an increment in the microparticles' hydrodynamic diameter as a result of the specific capturing of M-IgG onto the surface of the BSA-GtαM-IgG microparticles. For checking the cross-reactivity, rabbit immunoglobulin G (R-IgG) was used as a control. The hydrodynamic diameters of microparticles before and after addition of antigens were measured on a particle-by-particle basis by means of tunable resistive pulse sensing (TRPS) technique. The mean size of bare BSA-GtαM IgG microparticles was measured to be 1041.5 nm (n=180). Upon incubation with M IgG, the hydrodynamic diameter of particles showed a 16.4% increase to 1212.6 nm (Fig. 7). In contrast, the average hydrodynamic diameters of the microparticles remain almost the same value of 1071.5 nm after the addition of R IgG when compared with the bare BSA-GtαM-IgG microparticles. These results demonstrate protein microparticles composed of antibodies fabricated with the disulfide exchange reaction conserves specific binding affinity with target antigens. Moreover, the cross-reactivity study using R-IgG model shows insignificant non-specific interaction of the protein microparticles with non-specific target, which is important for potential future applications of such microparticles for bioseparation and target-specific drug delivery.

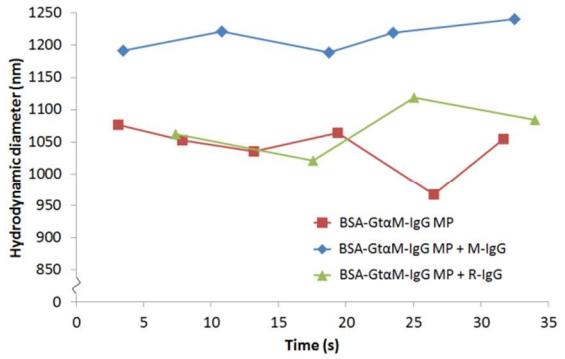

Fig. 7 Hydrodynamic diameter of BSA-GtαM-IgG microparticles as a function of time after incubation with specific antigen M-IgG (rhombus), non-specific antigen R-IgG (triangle) and blank control (square).

Biomaterials particularly in microparticle formulation are importance in both *in vitro* and *in vivo* applications such as for biotechnology (e.g. biocatalysis and bioseparation) and pharmaceutical applications. For *in vivo* application, the reducing environmental inside cells may facilitate the biodegradation of the disulfide-crosslinked protein microparticles. In fact, using degradable carriers such as liposome and albumin carries (e.g. nab-paclitaxel – albumin encapsulated paclitaxel) for *in vivo* drug delivery are desirable and was approved by FDA [36-37]. A highly stable non-degradable carrier may instead pose the possibility of carrier toxicity over a long period of time.

In addition, thiol chemistry has been widely used for immobilization of biomolecules such as enzymes and antibodies [38-39]. The reduction of native disulfide bonds prior to thiol immobilization may influence the enzyme activities depending on the accessibility of the disulfide bonds in the enzyme structure. In the state-of-the-art antibody labelling, the techniques are mainly based on chemical reduction of antibodies disulfide bonds producing reactive thiol group to couple with a fluorescence label. Therefore, our protein microparticle fabrication technique using glutathione-mediated disulfide exchange approach based on thiol chemistry could potentially applied to other existing enzymes and antibodies molecules that are suitable for thiol immobilization and conjugation techniques.

Conclusions

We have demonstrated a bioinspired green chemistry approach for the fabrication of protein microparticles based on peptide-mediated protein assembly via formation of intermolecular disulfide bonds. A redox reactive peptide, GSH, was used as a natural chemical to trigger the formation of intermolecular disulfide bonds with the inherent crosslinker (cysteine) of the protein molecules leads to the assembly of protein molecules into microparticle structure. The disulfide interchange reaction was proved by measuring the consumption of GSH. The protein microparticle was composed of assembled granular structures with size of tens of nanometers templated from the inter-connected porous of the $CaCO_3$ vaterite crystalline structure. We have further demonstrated this method is versatile to fabricate microparticles with various proteins such as BSA, enzymes (HRP) and antibodies (GtαM-IgG). Results from the enzyme kinetic studies and affinity assays suggested the biological functions of the resulting protein microparticles are highly conserved. By incorporating natural biomineral template such as spine with hierarchically organized structures, the presented approach may potentially apply for fabrication of complex protein structures for tissue engineering and regenerative medicine applications.

Acknowledgements

The authors would like to thank the kind supports from Materials Characterization and Preparation Facility of HKUST for technical assistance in SEM and microtome operations.

Notes and references

[a] *Department of Chemistry, Hong Kong University of Science and Technology, Clear Water Bay, Hong Kong, P.R. China. Tel: +852 23587410; E-mail: godfreylai@ust.hk*
[b] *Department of Physics, Chemistry and Biology, Biosensors and Bioelectronics Centre, Linköping University, 58183 Linköping, Sweden. Fax: +46 013287568; Tel: +46 013286921; E-mail: wing.cheung.mak@liu.se*

[c] *Department of Clinical and Experimental Medicine, Integrative Regenerative Medicine (IGEN) Centre, Linköping University, 58183 Linköping, Sweden. Fax: +46 013287568; Tel: +46 013286921; E-mail: wing.cheung.mak@liu.se*

† Electronic Supplementary Information (ESI) available: [details of any supplementary information available should be included here]. See DOI: 10.1039/b000000x/

‡ Footnotes should appear here. These might include comments relevant to but not central to the matter under discussion, limited experimental and spectral data, and crystallographic data.

1. X. Xu, H. Yu, S. Gao, H.-Q. Ma, K. W. Leong, and S. Wang, *Biomaterials*, 2002, **23**, 3765–3772.
2. K. K. Lai, R. Renneberg, and W. C. Mak, *Biosens. Bioelectron.*, 2012, **32**, 169–176.
3. W. C. Mak, H. Richter, A. Patzelt, W. Sterry, K. K. Lai, R. Renneberg, and J. Lademann, *Eur. J. Pharm. Biopharm.*, 2011, **79**, 23–27.
4. B. P. Chan, T. Y. Hui, C. W. Yeung, J. Li, I. Mo, and G. C. F. Chan, *Biomaterials*, 2007, **28**, 4652–4666.
5. L. Chiarantini, A. Cerasi, E. Millo, K. Sparnacci, M. Laus, M. Riccio, S. Santi, M. Ballestri, S. Spaccasassi, and L. Tondelli, *Int. J. Pharm.*, 2006, **324**, 83–91.
6. W. C. Mak, A. Patzelt, H. Richter, R. Renneberg, K. K. Lai, E. Rühl, W. Sterry, and J. Lademann, *J. Control. Release*, 2012, **160**, 509–14.
7. D. V. Volodkin, S. Schmidt, P. Fernandes, N. I. Larionova, G. B. Sukhorukov, C. Duschl, H. Möhwald, and R. von Klitzing, *Adv. Funct. Mater.*, 2012, **22**, 1914–1922.
8. S. Schmidt, M. Behra, K. Uhlig, N. Madaboosi, L. Hartmann, C. Duschl, and D. Volodkin, *Adv. Funct. Mater.*, 2012, **23**, 116–123.
9. D. Bingham, L. d. Juan, K. Tang, and A. Gomez, *J. Aerosol Sci.*, 1998, **29**, 561–574.
10. K. S. Suslick and M. W. Grinstaff, *J. Am. Chem. Soc.*, 1990, **112**, 7807–7809.
11. A. Ozkizilcik and K. Tuzlakoglu, *J. Tissue Eng. Regen. Med.*, 2012, DOI: 10.1002/term.1524.
12. L. Oner and M. J. Groves, *J. Pharm. Pharmacol.*, 1993, **45**, 866–870.
13. J. S. Pieper, T. Hafmans, J. H. Veerkamp, and T. H. van Kuppevelt, *Biomaterials*, 2000, **21**, 581–593.
14. G. Goissis, E. Marcantonio, R. A. Marcantônio, R. C. Lia, D. C. Cancian, and W. M. de Carvalho, *Biomaterials*, 1999, **20**, 27–34.
15. K. Ulubayram, E. Aksu, S. I. D. Gurhan, K. Serbetci, and N. Hasirci, *J. Biomater. Sci. Polym. Ed.*, 2002, **13**, 1203–1219.
16. P. A. Handford, A. K. Downing, D. P. Reinhardt, and L. Y. Sakai, *Matrix Biol.*, 2000, **19**, 457–470.
17. M. J. Sherratt, T. J. Wess, C. Baldock, J. Ashworth, P. P. Purslow, C. A. Shuttleworth, and C. M. Kielty, *Micron*, 2001, **32**, 185–200.
18. D. P. Reinhardt, J. E. Gambee, R. N. Ono, H. P. Bächinger, and L. Y. Sakai, *J. Biol. Chem.*, 2000, **275**, 2205–2210.
19. C. M. Kielty, C. Baldock, D. Lee, M. J. Rock, J. L. Ashworth, and C. A. Shuttleworth, *Philos. Trans. R. Soc. Lond. B. Biol. Sci.*, 2002, **357**, 207–217.
20. U. Berndorfer, H. Wilms, and V. Herzog, *J. Clin. Endocrinol. Metab.*, 1996, **81**, 1918–1926.
21. A. Schmitz, M. Klein, I. Gestmann, and V. Herzog, *Methods Enzymol.*, 2002, **348**, 306–313.
22. V. Herzog, U. Berndorfer, and Y. Saber, *J. Cell Biol.*, 1992, **118**, 1071–1083.
23. M. Terpstra, P.-G. Henry, and R. Gruetter, *Measurement of reduced glutathione (GSH) in human brain using LCModel analysis of difference-edited spectra.*, 2003, vol. 50.
24. M. Hepel, M. Stobiecka, J. Peachey, and J. Miller, in *Oxidative Stress: Diagnostics, Prevention, and Therapy*, American Chemical Society, 2011, vol. 1083, pp. 177–209 SE – 6.
25. J. D. Hayes and L. I. McLellan, *Free Radic. Res.*, 1999, **31**, 273–300.
26. J. Pizzorno and J. Katzinger, *J. Restor. Med.*, 2012, 24–37.
27. M. B. Toledano, C. Kumar, N. Le Moan, D. Spector, and F. Tacnet, *FEBS Lett.*, 2007, **581**, 3598–3607.
28. W. C. Mak, R. Georgieva, R. Renneberg, and H. Bäumler, *Adv. Funct. Mater.*, 2010, **20**, 4139–4144.
29. Q.-X. Zhang, R. Feng, W. Zhang, Y. Ding, J.-Y. Yang, and G.-H. Liu, *World J. Gastroenterol.*, 2005, **11**, 4451–4456.
30. L. Tartier, Y. L. McCarey, J. E. Biaglow, I. E. Kochevar, and K. D. Held, *Cell Death Differ.*, 2000, **7**, 1002–1010.
31. E. M. Pouget, P. H. H. Bomans, J. A. C. M. Goos, P. M. Frederik, G. de With, and N. A. J. M. Sommerdijk, *Science*, 2009, **323**, 1455–1458.
32. L. J. Brillson, in *Surfaces and Interfaces of Electronic Materials*, Wiley-VCH Verlag GmbH & Co. KGaA, Weinheim, Germany, 2010, pp. 279–304.
33. J. M. Yon, D. Perahia, and C. Ghélis, *Biochimie*, 1998, **80**, 33–42.
34. W. He, W.R. Newell, P.I. Haris, D. Chapman, J. Barber, *Biochemistry*, 1991, **30**, 4552-4559.
35. V. Chitarra, P. M. Alzari, G. A. Bentley, T. N. Bhat, J. L. Eiselé, A. Houdusse, J. Lescar, H. Souchon, and R. J. Poljak, *Proc. Natl. Acad. Sci. U. S. A.*, 1993, **90**, 7711–7715.
36. D. Peer, J.M. Karp, S. Hong, O.C. Farokhzad, R. Margalit, R. Langer, *Nature Technology*, 2007, **2**, 751-760.
37. B. Damascelli, G. Cantù, F. Mattavelli, P. Tamplenizza, P. Bidoli, E. Leo, F. Dosio, A.M. Cerrotta, G.D. Tolla, L.F. Frigerio, F. Garbagnati, R. Lanocita, A. Marchianò, G. Patelli, C. Spreafico, V. Tichà, V. Vespro, F. Zunino, *Cancer*, 2001, **92**, 2592-2602.
38. F. Rusmini, Z. Zhong, J. Feijen, *Biomacromolecules*, 2007, **8**, 1775-1789.
39. S.Y. Mao, J.M. Mullins, *Immunocytochemical Methods and Protocols*, 2009, **588**, 43-48.